

Continuations and bifurcations of relative equilibria for the positive curved three body problem

Toshiaki Fujiwara¹, Ernesto Pérez-Chavela²

¹College of Liberal Arts and Sciences, Kitasato University, Japan.
fujiwara@kitasato-u.ac.jp

²Department of Mathematics, ITAM, México.
ernesto.perez@itam.mx

Abstract

The positive curved three body problem is a natural extension of the planar Newtonian three body problem to the sphere \mathbb{S}^2 . In this paper we study the extensions of the Euler and Lagrange Relative equilibria (*RE* in short) on the plane to the sphere.

The *RE* on \mathbb{S}^2 are not isolated in general. They usually have one-dimensional continuation in the three-dimensional shape space. We show that there are two types of bifurcations. One is the bifurcations between Lagrange *RE* and Euler *RE*. Another one is between the different types of the shapes of Lagrange *RE*. We prove that bifurcations between equilateral and isosceles Lagrange *RE* exist for equal masses case, and that bifurcations between isosceles and scalene Lagrange *RE* exist for partial equal masses case.

Keywords Relative equilibria, Euler configurations, Lagrange configurations, cotangent potential.

Math. Subject Class 2020: 70F07, 70F10, 70F15

1 Introduction

A relative equilibrium for the Newtonian n -body problem, is a particular solution where the masses are rotating uniformly around their center of mass

with the same angular velocity. In these kind of motions the masses preserve their mutual distances for all time, that is, they behave as a rigid body motion. The fixed configuration at any time is called a central configuration. In the corresponding rotating frame they form an equilibrium point, from here the name [22, 17].

Since the central configurations are invariant under rotations and homotheties, we count classes of central configurations modulo these Euclidean transformations; then for $n = 3$, there are only 5 classes of relative equilibria, three collinear or Euler relative equilibria [10] and two equilateral triangle or Lagrange relative equilibrium [16].

The curved n -body problem is a natural extension of the classical Newtonian problem to spaces of constant curvature κ which could be positive or negative. For $n = 2$, the problem is divided into two classes, the Kepler problem (one particle is fixed, and the other one is moving according to it) and the 2-body problem (both masses are moving according to their mutual attractions). The first one is an old problem, introduced independently in the 1830's by J. Bolyai and N. Lovachevsky the codiscoverers of the first non-Euclidean geometries. The second one was introduced by Borisov et al [4, 5]. Unlike the Newtonian problem, on the sphere these problems are not equivalent, the first one is integrable and the second one is not [20].

In 1994, V.V. Kozlov showed that the cotangent potential is the natural way to extend the Newtonian potential to spaces of constant positive curvature [13]. In 2012, F. Diacu, E. Perez-Chavela and M. Santoprete [6], obtained the generalization of this problem in an unified way for any value of n and any value of the constant curvature κ . You can see [7] and [5] for a nice historical description of this problem.

In this paper we are interested in the analysis of relative equilibria for the two dimensional positive curved three body problem, which can be reduced to the analysis on the unit sphere $\mathbb{S}^2 \subset \mathbb{R}^3$. That is, we will study relative equilibria for three positive masses moving on \mathbb{S}^2 under the influence of the cotangent potential. From here on, just to simplify the notation we call to the relative equilibria simply as *RE*.

By exploiting the symmetries of some configurations and using spherical trigonometric arguments, several authors have found different families of *RE* on the sphere \mathbb{S}^2 see for instance [6, 7, 8, 9, 18, 19, 21, 23].

In a recent paper [11], the authors of this article developed a new systematic geometrical method to study *RE* on \mathbb{S}^2 , where the masses are moving on the sphere under the influence of a potential which only depends on the mutual distances among the masses, in particular for the cotangent potential.

For $n = 3$ the authors divide the analysis of RE on \mathbb{S}^2 in two big classes, the Euler relative equilibria (ERE by short) where the three masses are on the same geodesic, and the Lagrange relative equilibria (LRE by short), for the RE which are not in the previous class. In the same paper [11], the authors find the necessary and sufficient conditions on the shapes, to obtain ERE and LRE . In this paper we will restrict our analysis to the cotangent potential, that is, to the positive curved three body problem.

In [1], the authors proved that any RE of the planar n -body problem can be continued to spaces of constant curvature κ , positive or negative for small values of the parameter κ . This is a remarkable result, because for instance, it is well known that any three masses located at the vertices of an equilateral triangle generate a RE on the plane; however in the case of curved spaces, LRE with equilateral triangle shape only exist if the three masses are equal. In particular they show that any Lagrange relative equilibria can be continued to the sphere (the equilateral triangle shape, is not preserved in the continuation if the masses are not equal).

In this paper we will show that in general, we can continue a RE on the sphere, represented by an one dimensional curve. When two continuations of RE intersect, we call it a bifurcation, in the next section we will give the precise definition of these concepts.

After the introduction, the paper is organized as follows: In Section 2 we give the definitions of all concepts used along the paper, and we show how use the implicit function theorem to find the bifurcation points and the extensions of solutions. In Section 3 we do the analysis for the case of equal masses and in Section 4 we do the analysis for the case of partial equal masses. In section 5, we study LRE with general masses, and finally in Section 6 we summarize our results and state some final comments.

2 Conditions for a Shape

We consider three positive masses denoted by m_k moving on a sphere of radius R that we denote as \mathbb{S}^2 . The equations of motions are described by the Lagrangian, which in spherical coordinates (R, θ_k, ϕ_k) take the form,

$$L = R^2 \sum_k \frac{m_k}{2} (\dot{\theta}_k^2 + \dot{\phi}_k^2 \sin^2(\theta_k)) + \sum_{i,j} \frac{m_i m_j}{R} \frac{\cos \sigma_{ij}}{\sqrt{1 - \cos^2 \sigma_{ij}}}. \quad (1)$$

To facilitate the notations, we set $R = 1$ unless otherwise specified. We denote the angle of the minor arc on the great circle connecting the masses i

and j as σ_{ij} . In order to avoid singularities, we exclude the case $\cos^2 \sigma_{ij} = 1$, which corresponds to $\sigma_{ij} \neq 0, \pi$.

The above angles are related to each other by the relationship

$$\cos \sigma_{ij} = \cos \theta_i \cos \theta_j + \sin \theta_i \sin \theta_j \cos(\phi_i - \phi_j). \quad (2)$$

For the three-body problem, it is convenient to use the notation $\sigma_k = \sigma_{ij}$ for $(i, j, k) = (1, 2, 3), (2, 3, 1)$, and $(3, 1, 2)$. We define

$$\begin{aligned} U &= \{(\sigma_1, \sigma_2, \sigma_3) | 0 < \sigma_k < \pi\}, \\ U_{\text{phys}} &= \{(\sigma_1, \sigma_2, \sigma_3) \in U | \sigma_k \leq \sigma_i + \sigma_j \text{ and } \sum_k \sigma_k \leq 2\pi\}. \end{aligned} \quad (3)$$

The inequalities in U_{phys} are the conditions of σ_k to form a triangle. Note that one point in U_{phys} corresponds to two triangles with opposite orientation.

Definition 1. *A relative equilibrium is a solution of the equations of motion, which in spherical coordinates satisfies*

$$\dot{\theta}_k = 0 \quad \text{and} \quad \dot{\phi}_k = \omega \quad \text{for all } k = 1, 2, 3.$$

That is, a solution that behaves as if the masses belonged to a rigid body, the shape is the same for all time.

Remark 1. *Usually, people working on Geometric Mechanics define the RE as fixed points in a reduced system (see for instance [14] and the references therein). In other words, the RE are solutions which are invariant under the action of a continuous symmetric group G . In our case the symmetric group is $G = SO(3)$. The RE correspond to periodic orbits in the original phase space (the not reduced one), these periodic orbits are rotating uniformly around a principal axis. Then in order to determine a RE, we need to have the initial configuration and the angular velocity. If we express these conditions in the usual spherical coordinates, taking the rotation axis as the z -axis, we obtain Definition 1. By the other hand, if Definition 1 holds, then since $G = SO(3)$, we obtain that a RE is a fixed point in the reduced system. So, both definitions are equivalent.*

As we have seen in the previous Section, there are two kinds a RE on the sphere, *ERE* and *LRE*. In [11], we proved that the *ERE* must be on the equator or on a rotating meridian.

The big difficulty to study RE on the sphere is that the linear momentum and the center of mass are not more a first integral for the positive curved problem.

Fortunately in [11], we found that the center of mass can be substitute by the vanishing of two components of the angular momentum on the sphere.

To verify this fact, we observe that the Lagrangian is invariant under rotations around the centre of \mathbb{S}^2 , the angular momentum vector $\mathbf{c} = (c_x, c_y, c_z)$ is a first integral. The components of \mathbf{c} are

$$\begin{aligned} c_x &= R^2 \sum_k m_k \left(-\sin(\phi_k) \dot{\theta}_k - \sin(\theta_k) \cos(\theta_k) \cos(\phi_k) \dot{\phi}_k \right), \\ c_y &= R^2 \sum_k m_k \left(\cos(\phi_k) \dot{\theta}_k - \sin(\theta_k) \cos(\theta_k) \sin(\phi_k) \dot{\phi}_k \right), \\ c_z &= R^2 \sum_k m_k \sin^2(\theta_k) \dot{\phi}_k. \end{aligned}$$

Then, fixing the rotation axis as the z -axis, we obtain that the components $c_x = 0$ and $c_y = 0$ are integrals of motion.

Now by Definition 1, after the substitution $\dot{\theta}_k = 0$ and $\dot{\phi}_k(t) = \omega$, the angular momentum has the form $\mathbf{c} = (c_x, c_y, c_z) = (0, 0, c_z)$, where

$$\begin{aligned} (c_x, c_y) &= -R^2 \omega \sum_k m_k \sin(\theta_k) \cos(\theta_k) (\cos(\phi_k), \sin(\phi_k)), \\ c_z &= R^2 \omega \sum_k m_k \sin^2(\theta_k). \end{aligned} \tag{4}$$

We observe that taking $r_k = R\theta_k$ finite, in the limit $R \rightarrow \infty$ we obtain $\theta_k \rightarrow 0$, since $\theta_k = r_k/R \rightarrow 0$ for $R \rightarrow \infty$. Then, using equation (4), the expansion for $\cos \theta_k$ and $\sin \theta_k$ and dropping the higher order terms we obtain

$$c_x \rightarrow -R\omega \sum_k m_k r_k \cos(\phi_k) = 0 \quad \text{and} \quad c_y \rightarrow -R\omega \sum_k m_k r_k \sin(\phi_k) = 0. \tag{5}$$

Finally using the fact that $(c_x, c_y) = (0, 0)$, the above equation (5), is the condition to fix the center of mass at the origin on the Euclidean plane (see [11] for more details).

Remark 2. In [4] the authors use the reduction method to guarantee that the projections of the angular momentum of the system onto the original space

are preserved. Then by using Noether's theorem, they obtain the expressions of the above projections in Euler's angles. Due to the more classical geometric viewpoint that we discuss along this manuscript, we prefer to use our approach.

Using the two integrals $c_x = 0$ and $c_y = 0$, we prove that the problem to find RE on \mathbb{S}^2 is reduced to solve the eigenvalue problem $J\Psi_L = \lambda\Psi_L$ where J is an useful representation of the inertia tensor given by (see [11] for more details)

$$J = \begin{pmatrix} m_2 + m_3 & -\sqrt{m_1 m_2} \cos \sigma_3 & -\sqrt{m_1 m_3} \cos \sigma_2 \\ -\sqrt{m_2 m_1} \cos \sigma_3 & m_3 + m_1 & -\sqrt{m_2 m_3} \cos \sigma_1 \\ -\sqrt{m_3 m_1} \cos \sigma_2 & -\sqrt{m_3 m_2} \cos \sigma_1 & m_1 + m_2 \end{pmatrix}. \quad (6)$$

In the same paper [11], we show that the necessary and sufficient conditions to have LRE or ERE , can be described only in terms of m_k and σ_k , $k = 1, 2, 3$. The conditions for a shape to form LRE are

$$\begin{aligned} \lambda &= \frac{(m_2 + m_3) \sin^3(\sigma_1) - m_2 \cos(\sigma_3) \sin^3(\sigma_2) - m_3 \cos(\sigma_2) \sin^3(\sigma_3)}{\sin^3(\sigma_1)} = \lambda_1 \\ &= \frac{(m_3 + m_1) \sin^3(\sigma_2) - m_3 \cos(\sigma_1) \sin^3(\sigma_3) - m_1 \cos(\sigma_3) \sin^3(\sigma_1)}{\sin^3(\sigma_2)} = \lambda_2 \\ &= \frac{(m_1 + m_2) \sin^3(\sigma_3) - m_1 \cos(\sigma_2) \sin^3(\sigma_1) - m_2 \cos(\sigma_1) \sin^3(\sigma_2)}{\sin^3(\sigma_3)} = \lambda_3. \end{aligned} \quad (7)$$

Let λ_{ij} be the difference of λ_i and λ_j , namely

$$\lambda_{ij} = \lambda_i - \lambda_j. \quad (8)$$

Then, the condition for have a LRE is equivalent to $\lambda_{12} = \lambda_{23} = 0$.

The correspondence between the solution $\sigma_k \in U_{\text{phys}}$ of this condition and the configuration variables θ_k is given by

$$\cos \theta_k = s \sqrt{M - \lambda} \sin^3(\sigma_k) / \sqrt{\sum_{\ell} m_{\ell} \sin^6(\sigma_{\ell})}. \quad (9)$$

Then using σ_k and θ_k , equation (2) determines $\cos(\phi_i - \phi_j)$. Where $M = \sum_{\ell} m_{\ell}$ is the total mass, and $s = \pm 1$. If we take $s = 1$ the three masses are on the northern hemisphere, when $s = -1$ they are on southern hemisphere. Finally, the angular velocity is given by

$$\omega^2 = \frac{\sum_{\ell} m_{\ell} \sin^6(\sigma_{\ell})}{\sin^3(\sigma_1) \sin^3(\sigma_2) \sin^3(\sigma_3)}. \quad (10)$$

Thus, the problem to find a configuration of *LRE* is reduced to find the solution σ_k of the condition $\lambda_{12} = \lambda_{23} = 0$ (See [11] for more details).

Similarly, the necessary and sufficient condition for a shape to form an *ERE* on a rotating meridian with $\sigma_3 = \sigma_1 + \sigma_2$, namely the mass m_3 is located between m_1 and m_2 , is

$$d = \frac{m_1 \sin(2\sigma_2) - m_2 \sin(2\sigma_1)}{\sin^2 \sigma_3} + \frac{m_2 \sin(2\sigma_3) + m_3 \sin(2\sigma_2)}{\sin^2 \sigma_1} - \frac{m_3 \sin(2\sigma_1) + m_1 \sin(2\sigma_3)}{\sin^2 \sigma_2} = 0. \quad (11)$$

You can consult reference [11] for the correspondence between σ_k and the configuration variables θ_k, ω^2 .

The conditions for a shape to form an *ERE* on the equator $\sigma_1 + \sigma_2 + \sigma_3 = 2\pi$ are

$$\mu_k < \mu_i + \mu_j \quad (i, j, k) \text{ is a permutation of } (1, 2, 3), \quad (12)$$

where $\mu_k = \sqrt{m_i m_j}$. For this case, σ_k is given by

$$\sigma_k = \arccos \left(\frac{\mu_k^2 - \mu_i^2 - \mu_j^2}{2\mu_i \mu_j} \right). \quad (13)$$

Note that there is just one set of σ 's (two shapes with different orientation) for given masses. For the *LRE* and the *ERE* on a rotating meridian on the sphere, we will show that some of these *RE* can be continued into the three dimensional space given by $(\sigma_1, \sigma_2, \sigma_3)$, and that these continuations can meet in this space. We call this ‘‘bifurcation’’, to be more precise we define:

Definition 2. *A bifurcation point of LRE and ERE on a rotating meridian is a point on a plane $\sigma_k = \sigma_i + \sigma_j$, where the continuation of a LRE and an ERE coincide. This bifurcation point is a coupling where two continuations of LRE with opposite orientation connected.*

We will show ahead in this paper, that some *LRE* meets *ERE* on the equator, and since an *ERE* on the equator is just one point for given mass ratio and given orientation, we define:

Definition 3. *An Euler coupling on the Equator is a point with $\sigma_1 + \sigma_2 + \sigma_3 = 2\pi$, where two continuations of LRE with the same orientation, one on the northern and the other one on the southern hemisphere, connected.*

Finally we have that the shapes of *LRE* can be grouping into equilateral, isosceles, and scalene triangles. We will show that for equal masses case, $m_1 = m_2 = m_3$, equilateral and isosceles *LRE* have continuation. When only two masses are equal, for instance $m_1 = m_2 \neq m_3$, we have continuation of isosceles and scalene *LRE*. We define the bifurcation point as follows.

Definition 4. *Let the set $\{A, B\}$ be one of $\{\text{equilateral, isosceles}\}$ or $\{\text{isosceles, scalene}\}$ *LRE*. A bifurcation point between A and B is the intersection point of the continuation of A and B .*

The existence of bifurcation points between *LRE* one in the group A and other in the group B can be understood by two simple but important properties of the surfaces defined by $\lambda_{ij} = 0$ in U_{phys} .

Property 1. *For $\sigma_i = \sigma_j$,*

$$\lambda_{ij} = (m_i - m_j)(\cos \sigma_k - 1). \quad (14)$$

From this property we obtain the following proposition and corollaries whose proofs are obvious.

Proposition 1. *The necessary condition for *LRE* with $\sigma_i = \sigma_j$ is $m_i = m_j$.*

Corollary 1. *Unequal masses implies scalene triangle *LRE*.*

Corollary 2. *Equilateral triangle *LRE* needs $m_1 = m_2 = m_3$.*

Property 2. *For $m_i = m_j$, the function $\lambda_{ij}(\sigma_i, \sigma_j, \sigma_k)$ is an anti-symmetric function of σ_i and σ_j , and can be factorized as*

$$\lambda_{ij}(\sigma_i, \sigma_j, \sigma_k) = \frac{\sin(\sigma_i - \sigma_j)}{\sin^3(\sigma_i) \sin^3(\sigma_j)} \tilde{\lambda}_{ij}(\sigma_i, \sigma_j, \sigma_k), \quad (15)$$

where

$$\begin{aligned} \tilde{\lambda}_{ij}(\sigma_i, \sigma_j, \sigma_k) = & \nu_k \cos(\sigma_k) \sin(\sigma_i + \sigma_j) \left(\sin^4(\sigma_i) + \sin^2(\sigma_i) \sin^2(\sigma_j) + \sin^4(\sigma_j) \right) \\ & - \frac{\sin^3(\sigma_k)}{4} \left(\cos(3\sigma_i + \sigma_j) + \cos(\sigma_i + 3\sigma_j) - 2 \cos(\sigma_i + \sigma_j) \right), \end{aligned}$$

$$\text{and } \nu_k = \frac{m_i}{m_k} = \frac{m_j}{m_k}.$$

(16)

This property explains the existence of bifurcation points between two groups of shapes of *LRE*.

We explain why for $m_1 = m_2 \neq m_3$ we obtain a bifurcation point of isosceles *LRE* and scalene *LRE*. For this case, the surface $\lambda_{12} = 0$ is split into the plane $\sigma_1 = \sigma_2$, and the surface $\tilde{\lambda}_{12} = 0$ by Property 2. Then, the condition for *LRE*, $\lambda_{12} = \lambda_{23} = 0$, is split into two cases, intersection of $\sigma_1 = \sigma_2$ and $\lambda_{23} = 0$ namely isosceles *LRE*, and intersection of $\tilde{\lambda}_{12} = 0$ and $\lambda_{23} = 0$, namely scalene *LRE*. Then, the intersection of the three surfaces $\sigma_1 = \sigma_2$ and $\tilde{\lambda}_{12} = 0$ and $\lambda_{23} = 0$ gives the bifurcation points.

Similarly, there are bifurcation points of equilateral *LRE* and isosceles *LRE* for the equal masses case, $m_1 = m_2 = m_3$.

We will use the implicit function theorem to study bifurcations. By this theorem, if two continuous differentiable functions $f(x, y, z)$ and $g(x, y, z)$ have a solution $f(x_0, y_0, z_0) = g(x_0, y_0, z_0) = 0$, and $\nabla f \times \nabla g \neq 0$ at (x_0, y_0, z_0) , then a continuation of the solution $f = g = 0$ from this point exists in some finite interval. A geometrical interpretation of this theorem is that the conditions $f = g = 0$ and $\nabla f \times \nabla g \neq 0$ means that the two surfaces intersect at this point and the vector $\nabla f \times \nabla g$ represents the tangent vector of the intersection curve at this point.

3 Equal masses case

As shown in Property 2, the conditions for have a *LRE*, $\lambda_{12} = 0$ and $\lambda_{23} = 0$ are split into $(\sigma_1 = \sigma_2$ or $\tilde{\lambda}_{12} = 0)$ and $(\sigma_2 = \sigma_3$ or $\tilde{\lambda}_{23} = 0)$.

First we will show that there are no scalene *LRE* (intersection of $\tilde{\lambda}_{12} = 0$ and $\tilde{\lambda}_{23} = 0$), then we describe the equilateral $(\sigma_1 = \sigma_2$ and $\sigma_2 = \sigma_3)$ and isosceles *LRE* $(\sigma_1 = \sigma_2$ and $\tilde{\lambda}_{23} = 0$ or $\sigma_2 = \sigma_3$ and $\tilde{\lambda}_{12} = 0)$ and the bifurcation between them.

3.1 No scalene *LRE*

Theorem 1. *There are no scalene *LRE* for the equal masses case.*

Proof. We will show a contradiction if we assume that there is a scalene *LRE* with $(\sigma_1, \sigma_2, \sigma_3) = (x, y, z)$. Let be $\tilde{\lambda}_{12} = g(\sigma_1, \sigma_2, \sigma_3)$, then $\tilde{\lambda}_{23} = g(\sigma_2, \sigma_3, \sigma_1)$ and $\tilde{\lambda}_{31} = g(\sigma_3, \sigma_1, \sigma_2)$. Since, this is a scalene triangle, (x, y, z) must satisfies $g(x, y, z) = g(y, z, x) = g(z, x, y) = 0$. By the definition of the function g , it is symmetric for the first two variables. Therefore, g must be zero for any permutation of (x, y, z) if the assumption is true.

Now, define $g_0 = g$ and g_n for $n = 1, 2, 3$ by

$$\begin{aligned} g_0(x, y, z) - g_0(x, z, y) &= 2 \sin(y - z)g_1(x, y, z), \\ g_1(x, y, z) - g_1(y, x, z) &= -2(\cos x - \cos y)g_2(x, y, z), \\ g_2(x, y, z) - g_2(x, z, y) &= 16(\cos y - \cos z)g_3(x, y, z). \end{aligned} \quad (17)$$

Since $g_0 = 0$ for any permutations of (x, y, z) and $\sin(y - z) \neq 0$, $g_1 = 0$ for any permutations of (x, y, z) . Similarly, $g_2 = g_3 = 0$. Here, the function g_3 is a totally symmetric function of (x, y, z) ,

$$\begin{aligned} g_3(x, y, z) &= \left(3 - \cos(2x) - \cos(2y) - \cos(2z)\right) \\ &\quad \cos\left((x + y)/2\right) \cos\left((y + z)/2\right) \cos\left((z + x)/2\right). \end{aligned} \quad (18)$$

The possible solutions of $g_3 = 0$ are $x + y = \pi$ or $y + z = \pi$ or $z + x = \pi$. However

$$g(x, y, z)|_{x+y=\pi} = \frac{1}{2} \left(\cos(2x) - 1 \right) \sin^3(z) \neq 0. \quad (19)$$

Similarly $g(y, z, x)|_{y+z=\pi} \neq 0$, and $g(z, x, y)|_{z+x=\pi} \neq 0$. This is the contradiction we are looking for. \square

3.2 Isosceles and equilateral *LRE*

In this subsection, we consider the shape with $\sigma_1 = \sigma_2 = \sigma$. So,

$$U = (0, \pi)^2, \quad U_{\text{phys}} = \{(\sigma, \sigma_3) \in U \mid \sigma_3 \leq 2\sigma \text{ and } \sigma_3 \leq 2(\pi - \sigma)\}. \quad (20)$$

The isosceles solution is the solution of

$$\begin{aligned} g(\sigma, \sigma_3) &= g(\sigma_3, \sigma, \sigma) \\ &= \cos(\sigma) \left(\sin^4(\sigma) + \sin^2(\sigma) \sin^2(\sigma_3) + \sin^4(\sigma_3) \right) \\ &\quad + \frac{\sin^3(\sigma)}{2} \left(\cos(\sigma + \sigma_3) - \cos(\sigma - \sigma_3) \cos(2(\sigma + \sigma_3)) \right) = 0. \end{aligned} \quad (21)$$

Obviously $g(\pi - \sigma, \pi - \sigma_3) = g(\sigma, \sigma_3)$.

Proposition 2. *The bifurcation points between equilateral *LRE* and isosceles *LRE* are $\sigma_k = \sigma_c$ and $\sigma_k = \pi - \sigma_c$, where $\sigma_c = 2^{-1} \arccos(-4/5) = 1.249\dots$ (see Figure 1).*

Proof. The bifurcation points are the solutions of

$$g(\sigma, \sigma) = \sin^5(\sigma) \left(4 + 5 \cos(2\sigma) \right) = 0. \quad (22)$$

\square

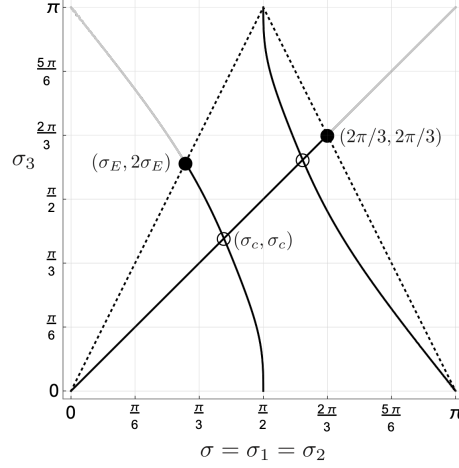


Figure 1: Equilateral *LRE* (the straight line) and isosceles *LRE* (two curves). Two points with hollow circle are the bifurcation points of equilateral and isosceles. The dotted lines represents the boundary of U_{phys} . The end points shown by the black circles are Euler *RE*. The point $(\sigma_E, 2\sigma_E)$ is the bifurcation point of *LRE* and *ERE*.

Proposition 3. *The end points of an equilateral LRE, $\sigma_k = 2\pi/3$, $k = 1, 2, 3$, is the ERE on the equator. The end point of isosceles LRE, $p_E = (\sigma_E, 2\sigma_E)$ with*

$$\sigma_E = \arccos(2^{-3/4}) = 0.934\dots \quad (23)$$

is the ERE on a rotating meridian.

Proof. The former is obvious. The latter is the solution of

$$g(\sigma, 2\sigma) = 2 \cos(\sigma) \sin(\sigma)^5 \left(3 + 2 \cos(2\sigma) \right) \left(2 + 4 \cos(2\sigma) + \cos(4\sigma) \right) = 0. \quad (24)$$

□

The point p_E is the bifurcation point between isosceles *LRE* and *ERE* on a rotating meridian. We will consider this bifurcation point in the next section.

Remark 3. *Although the points $\sigma_k = 2\pi/3$ and p_E are the end points of LRE in U_{phys} , they are not the end points of configurations of LRE, they are just the coupling points. Remember the definitions 2 and 3.*

4 Partial equal masses case

In this section, we consider the case $m_1 = m_2 = m_3\nu$, with $\nu > 0$.

As shown in Property 2, the condition $\lambda_{12} = 0$ is reduced to $\sigma_1 = \sigma_2$ or $\tilde{\lambda}_{12} = 0$. In the next subsection, we consider the first case, isosceles *LRE* (intersection of $\sigma_1 = \sigma_2$ and $\lambda_{23} = 0$). The subsection 4.1.2 is devoted to the bifurcation of isosceles *LRE* and isosceles *ERE*. The second case, ($\tilde{\lambda}_{12} = 0$ and $\lambda_{23} = 0$) describes scalene *LRE*. In subsection 4.2, we will treat the bifurcation of isosceles *LRE* and scalene *LRE* ($\sigma_1 = \sigma_2$ and $\tilde{\lambda}_{12} = 0$ and $\lambda_{23} = 0$).

4.1 Isosceles *LRE*

Let be $\sigma = \sigma_1 = \sigma_2$, then U and U_{phys} take the same form as in (20).

4.1.1 Mass ratio for a given shape

Let be

$$\alpha(\sigma, \sigma_3) = (1 + \cos \sigma_3) \sin^3(\sigma_3) - 2 \cos(\sigma) \sin^3(\sigma), \quad (25)$$

$$\beta(\sigma, \sigma_3) = \sin^3(\sigma) - \cos(\sigma) \sin^3(\sigma_3). \quad (26)$$

A simple calculation proves that the solutions of $\alpha = \beta = 0$ are, the point $(\sigma_E, 2\sigma_E)$ in U_{phys} , and the points $(0, 0)$ and $(0, \pi)$ on the boundary of U . Where, σ_E is defined by (23). See Figure 2.

Then the following proposition follows.

Proposition 4. *For $m_1 = m_2$, any point (σ, σ_3) in U_{phys} with $\alpha\beta > 0$ forms an isosceles *LRE* by choosing suitable ν .*

Proof. For this case, $\lambda_{12} = 0$ is satisfied. Therefore, the condition for *LRE* is

$$\lambda_{23} = -\nu\alpha/\sin^3(\sigma_3) + \beta/\sin^3(\sigma) = 0. \quad (27)$$

Therefore, if $\alpha \neq 0$ and $\beta \neq 0$,

$$\nu = \frac{\sin^3(\sigma_3)\beta(\sigma, \sigma_3)}{\sin^3(\sigma)\alpha(\sigma, \sigma_3)}. \quad (28)$$

This equation defines ν in terms of (σ, σ_3) uniquely, and $\nu > 0$ demands $\alpha\beta > 0$. In fact, the region $\alpha\beta > 0$ in U_{phys} is the region where $\alpha > 0$ and $\beta > 0$. \square

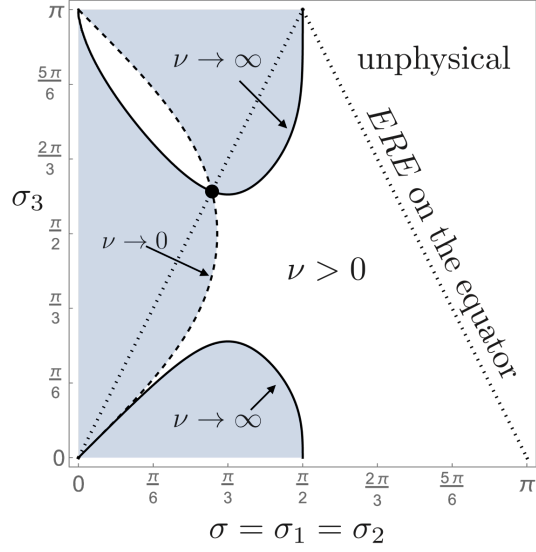


Figure 2: The contours of $\alpha = 0$ (solid curves) and $\beta = 0$ (dashed curve) represent the mass ratio $\nu \rightarrow \infty$ and $\nu \rightarrow 0$ respectively. The white and grey regions represent $\alpha\beta$ is positive or negative, respectively. The two dotted straight lines represents the boundary of U_{phys} . The dotted line $\sigma_3 = 2\pi - 2\sigma$ represents isosceles ERE on the equator. See Proposition 6. For any point (σ, σ_3) in the white region inside the two lines, there is a unique suitable mass ratio ν for which isosceles LRE exist. In the grey region, isosceles LRE do not exist for any choice of positive masses. See Proposition 4. The point $(\sigma_E, 2\sigma_E)$ shown in the black circle, represents the isosceles ERE on a rotating meridian for any mass ratio ν . See Propositions 5 and 7.

The next result follows immediately from equation (27).

Proposition 5. *The shape $(\sigma_E, 2\sigma_E)$ that makes $\alpha = \beta = 0$ satisfies the condition for *LRE* for any ν .*

Actually this shape is an *ERE* on a rotating meridian. Therefore, it corresponds to the bifurcation point of *LRE* and *ERE*, that is, we can pass from a *LRE* to an *ERE* or vice versa.

Proposition 6 (Euler coupling). *On the line $\sigma_3 = 2\sigma$, only $\sigma = \sigma_E$ satisfies the condition for *LRE* with any ν . On the other hand, on the line $\sigma_3 = 2\pi - 2\sigma$, any point in $\pi/2 < \sigma < \pi$ satisfies the condition for *LRE* choosing suitable $\nu < 4$.*

Proof. On the line $\sigma_3 = 2\sigma$, $\alpha = 2 \sin^3(\sigma) \cos(\sigma)(8 \cos^4(\sigma) - 1)$ and $\beta = \sin^3(\sigma)(1 - 8 \cos^4(\sigma))$. Therefore, $\alpha\beta < 0$ if $\sigma \neq \sigma_E$, and $\alpha = \beta = 0$ if $\sigma = \sigma_E$.

On the other hand, on the line $\sigma_3 = 2\pi - 2\sigma$, $\alpha = -2 \cos(\sigma) \sin^3(\sigma)(1 + 8 \cos^4(\sigma))$ and $\beta = \sin^3(\sigma)(1 + 8 \cos^4(\sigma))$. Therefore $\alpha\beta > 0$ because $\pi/2 < \sigma < \pi$. For this case, $\nu = 4 \cos^2(\sigma) < 4$. This shape is the *ERE* on the equator. And the inequality $\nu < 4$ is exactly the same as the condition (12) for *ERE* on the equator. \square

4.1.2 Bifurcation point between isosceles *LRE* and isosceles *ERE*

Proposition 7. *The shape $(\sigma_E, 2\sigma_E)$ is the unique bifurcation point between isosceles *LRE* and isosceles *ERE*.*

Proof. In the previous Proposition we have already proved that the shape $p_E = (\sigma_E, 2\sigma_E)$ is the Euler coupling of isosceles *LRE*. Obviously, the shape p_E is an *ERE* on the rotating meridian, and then, continuation from this shape of isosceles *ERE* for any $\nu > 0$ does exist.

The proof of the existence of the continuation of a *LRE* for any ν is given by showing that $\nabla\lambda_{23}|_{p_E} \neq 0$. In fact,

$$\begin{aligned} \nabla\lambda_{23}|_{p_E} &= \left(-\frac{\nu\nabla\alpha}{\sin^3(\sigma_3)} + \frac{\nabla\beta}{\sin^3(\sigma)} \right) \Big|_{p_E} \\ &= \left(\frac{2^{5/4}(1 + \sqrt{2} + \nu(\sqrt{2} - 1))}{\sqrt{4 - \sqrt{2}}}, \frac{2^{1/4}(3(\sqrt{2} - 1) + \nu(5 - 2\sqrt{2}))}{\sqrt{4 - \sqrt{2}}} \right) \end{aligned} \quad (29)$$

$\neq 0$ for any $\nu > 0$.

By the implicit function theorem, there is a continuation of *LRE* from p_E . \square

4.1.3 Isosceles *LRE* for the restricted three-body problem

Here we consider the isosceles *LRE* in the restricted problem with $m_1 = m_2$ finite and $m_3 \rightarrow 0$. The size dependence will be interesting.

The isosceles *LRE* for this limit are represented by the $\nu \rightarrow \infty$ curve in Figure 2, since $\nu = m_1/m_3 = m_2/m_3$. As we can see, there are two curves where $\nu \rightarrow \infty$, one connects $(0, 0)$ and $(\pi/2, 0)$, and the other connects $(\sigma_E, 2\sigma_E)$ and $(\pi/2, \pi)$.

Now, trace the isosceles *LRE* with respect to $\sigma = \sigma_1 = \sigma_2 \in (0, \pi/2)$. For sufficiently small σ , there is one *LRE* shape that is almost equilateral. Note that one shape in (σ, σ_3) represents four *LRE* configurations, two for orientations of the triangle, and two for the places near the north pole or south pole. So, there are four *LRE* configurations for $0 < \sigma < \sigma_E$. Then at $\sigma = \sigma_E$, new *LRE* shape bifurcated from $(\sigma_E, 2\sigma_E)$. So, there are eight *LRE* configurations for $\sigma_E < \sigma < \pi/2$.

With respect to $\sigma_3 \in (0, \pi/2)$, the situation is more complex. Note that the graph $\alpha(\sigma, \sigma_3) = 0$, takes the local minimum and maximum for σ_3 at $\sigma = \pi/3$, where the minimum and maximum value of σ_3 are the solution of $\alpha(\pi/3, \sigma_3) = (1 + \cos(\sigma_3)) \sin^3(\sigma_3) = (\sqrt{3}/2)^3$. The solutions are $\sigma_3 = \sigma_s = 0.81\dots$ (the local maximum), and $\sigma_\ell = 1.84\dots$ (the local minimum). So, the range $\sigma_3 \in (0, \pi/2)$ is divided into four pieces by the three values $\sigma_3 = \sigma_s, \sigma_\ell, 2\sigma_E$. As shown in Figure 2, in the interval $\sigma_3 \in (\sigma_s, \sigma_\ell)$, there are no isosceles *LRE* for the restricted problem.

4.2 Bifurcation points between isosceles *LRE* and scalene *LRE*

In this subsection, we will show the existence of the bifurcations between isosceles *LRE* with $\sigma_1 = \sigma_2$ and scalene *LRE*. As described in the section 2, the bifurcation point of this type is the intersection of three surfaces, $\sigma = \sigma_1 = \sigma_2$, $\tilde{\lambda}_{12} = 0$, and $\lambda_{23} = 0$.

Now, since

$$\tilde{\lambda}_{12}(\sigma, \sigma, \sigma_3) = \sin^2(\sigma) \left(6\nu \sin^3(\sigma) \cos(\sigma) \cos(\sigma_3) + (1 + 2 \cos(2\sigma)) \sin^3(\sigma_3) \right), \quad (30)$$

we obtain that $\tilde{\lambda}_{12}(\sigma, \sigma, \sigma_3) = 0$ is equivalent to

$$6\nu \sin^3(\sigma) \cos(\sigma) \cos(\sigma_3) + (1 + 2 \cos(2\sigma)) \sin^3(\sigma_3) = 0. \quad (31)$$

On the other hand, $\lambda_{23}(\sigma, \sigma, \sigma_3) = 0$ determines ν by equation (28). Substituting this ν into the equation (31), we get the equation for the set of

$\tilde{\lambda}_{12} = \lambda_{23} = 0$ and $\sigma = \sigma_1 = \sigma_2$,

$$j(\sigma, \sigma_3) = (1 + 2 \cos(2\sigma)) \sin^3(\sigma_3) + \frac{6 \cos(\sigma) \cos(\sigma_3) (\sin^3(\sigma) - \cos(\sigma) \sin^3(\sigma_3))}{1 + \cos(\sigma_3) - 2 \cos(\sigma) \sin^3(\sigma) / \sin^3(\sigma_3)}$$

$$= 0. \tag{32}$$

Unfortunately, we don't have a proof that almost all points on the curve $j(\sigma, \sigma_3) = 0$ have a continuation of scalene *LRE*. But we are able to give a proof for two points.

Example 1. *The points $p_a = (\pi/3, \pi/2)$ and $p_b = (2\pi/3, \pi/2)$ are bifurcation points between isosceles and scalene *LRE*.*

Proof. It is not difficult to verify that the points p_a and p_b satisfy the condition $j = 0$. In fact the point p_a corresponds to an isosceles *LRE* for $\nu = 8(36 - 5\sqrt{3})/333$. For $\nabla = (\partial_{\sigma_1}, \partial_{\sigma_2}, \partial_{\sigma_3})$, the vector $\nabla \tilde{\lambda}_{12}(\sigma_1, \sigma_2, \sigma_3) \times \nabla \lambda_{23}(\sigma_1, \sigma_2, \sigma_3) = 3\sqrt{3} \nu/8 (1, -1, 0)$ indicates the scalene direction, and the vector $\nabla(\sigma_1 - \sigma_2) \times \nabla \lambda_{23} = (-\nu, -\nu, 8/3)$ indicates the isosceles direction. By the implicit function theorem, there are continuation of scalene *LRE* and isosceles *LRE* from p_a .

Similarly, p_b corresponds to an isosceles *LRE* for $\nu = 8(36 + 5\sqrt{3})/333$. In this case the corresponding vectors are $\nabla \tilde{\lambda}_{12} \times \nabla \lambda_{23} = 3\sqrt{3} \nu/8 (-1, 1, 0)$ and $\nabla(\sigma_1 - \sigma_2) \times \nabla \lambda_{23} = (-\nu, -\nu, 8/3)$. \square

In subsection 4.3.2, we will give a numerical result that shows that there are continuation of scalene *LRE* from the points on $j = 0$ except for three exceptional points.

4.3 Numerical results

In this subsection we present numerical simulations which show some continuations of *RE*.

4.3.1 Isosceles *LRE*

The result of the numerical calculations are shown in Figure 3. The contours represent curves for ν a positive constant. The white region in this figure represents $\nu > 0$. The gray region is $\nu < 0$ or outside of U_{phys} . Every contour with $\nu \neq 1$ has a unique continuation from an edge to another edge of U .

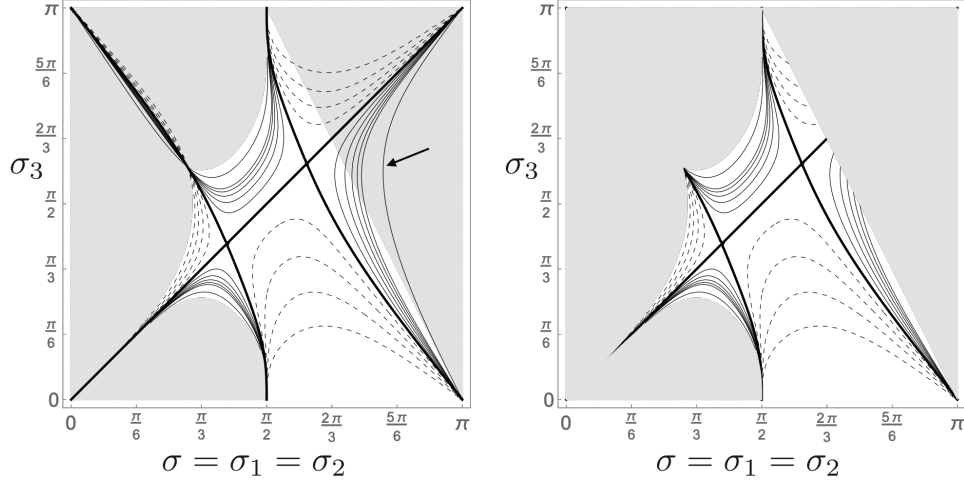


Figure 3: Contours for $\nu =$ a positive constant in the (σ, σ_3) plane. The left and right pictures represent the contours in U and U_{phys} respectively. The thick contour represents $\nu = 1$. The dashed contours are for $\nu = 0.2, 0.4, \dots, 0.8$, and solid contours are for $\nu = 1.2, 1.4, \dots, 1.8, 2, 4$. Note that the rightmost contour for $\nu = 4$ (pointed by an arrow) in U is outside of U_{phys} .

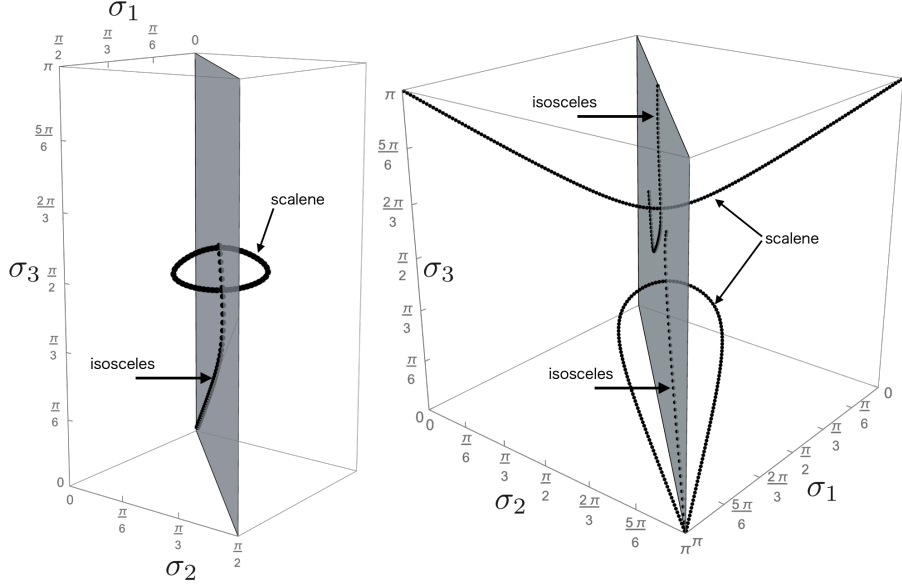
The 0-*LRE* continuations for $\nu > 0$ are emerging from the origin as showed above, it looks close to a straight line. The end points of this continuation are $(\sigma, \sigma_3) = (\sigma_E, 2\sigma_E)$ for $\nu < 1$, and $(\sigma, \sigma_3) = (\pi/2, 0)$ (binary collision) for $\nu > 1$.

Figure 3 shows that the continuation of *LRE* for any $\nu > 0$ are emerging form $(\sigma_E, 2\sigma_E)$, which is the unique bifurcation point between *LRE* and *ERE* for $m_1 = m_2$ case.

In Figure 3, we can see the Euler couplings on the line $2\sigma + \sigma_3 = 2\pi$, which is the *ERE* on the equator. Note that the curve $\nu = 4$ (the rightmost solid curve in the left side of Figure 3) is outside of U_{phys} , as shown in Proposition 6. All the other end points $(\pi/2, 0)$, $(\pi, 0)$ and $(\pi/2, \pi)$ correspond to collision.

4.3.2 Bifurcation between isosceles *LRE* and scalene *LRE*

Figure 4 shows two examples of bifurcations between isosceles *LRE* and scalene *LRE* for $\nu = 8(36 \pm 5\sqrt{3})/333$ which were described in Example 1. For each mass ratio, two bifurcation pints exists. For $\nu = 8(36 - \sqrt{3})/333$, the



x

Figure 4: Two examples for bifurcation of isosceles *LRE* and scalene *LRE* for $m_1 = m_2 \neq m_3$. The dotted curves represent the continuation of isosceles *LRE*. The solid curves represent the continuations of scalene *LRE*. The grey plane is $\sigma_1 = \sigma_2$, where the isosceles continuations lay on. The scalene continuations intersect this plane. Left: For $\nu = 8(36 - 5\sqrt{3})/333$, two bifurcation points exist: $(\sigma_1, \sigma_2, \sigma_3) = (\pi/3, \pi/3, \pi/2)$, and $(0.942\dots, 0.942\dots, 1.850\dots)$. The scalene curve is a loop, and it crosses the isosceles curve at two points. The isosceles curve is the 0-*LRE* continuation. Right: For $\nu = 8(36 + 5\sqrt{3})/333$, we also have two bifurcation points of isosceles and scalene, at $(2\pi/3, 2\pi/3, \pi/2)$, and $(1.764\dots, 1.764\dots, 2.078\dots)$. For this mass ratio, however, as shown in this picture, the bifurcation points are on separate curves.

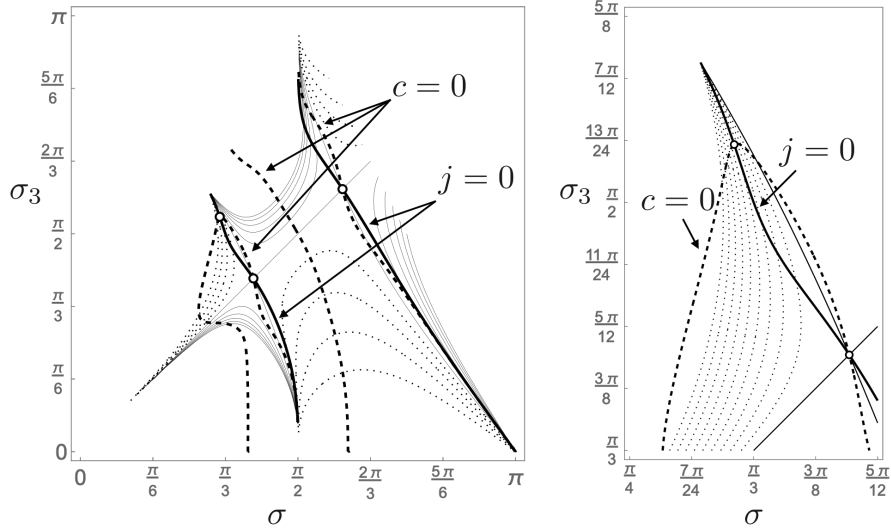


Figure 5: The bifurcation points of isosceles *LRE* ($\sigma = \sigma_1 = \sigma_2$) and scalene *LRE*. The thick curves represent the set of bifurcation points, $j = 0$. Thin dotted or solid curves represents $\nu = \text{constant}$ contour. The points on $j = 0$ are the bifurcation point if $c = \nabla \tilde{\lambda}_{12} \times \nabla \lambda_{23} \neq 0$. The curve $c = 0$ is shown by the thick dashed curves. Left: The global view. The three points represented by the hollow circle satisfy $j = c = 0$ in U_{phys} . Right: A close-up view.

continuation of scalene *LRE* is a closed loop as shown in the left side of figure 4. The loop intersects one continuation curve of the isosceles continuation twice. This isosceles continuation is the *0-LRE* continuation. For $\nu = 8(36 + \sqrt{3})/333$, we also get two bifurcation points. In this case, two scalene continuation curves intersect two different continuation of isosceles curves. See the right side of Figure 4.

Figure 5 shows the global structure of the bifurcation point of this type. The points on the curve $j = 0$ give the bifurcation points if $c = \nabla \tilde{\lambda}_{12} \times \nabla \lambda_{23} \neq 0$. The curve $c = 0$ is also shown in the same figure.

We can see in this figure, that the bifurcations occur for $|\nu - 1|$ sufficiently small. That is, the bifurcation from *0-LRE* continuation is only possible if $\nu = 1 - \delta$ with sufficiently small $\delta > 0$. In the following we will show numerically how small could be ν .

On the cross point of $j = 0$ and $c = 0$ the bifurcation doesn't occur, namely, no continuation of scalene solutions exists. Figure 5 shows that there are three such points. The points $(\sigma, \sigma_3) = (\sigma_c, \sigma_c)$, $(\pi - \sigma_c, \pi - \sigma_c)$,

correspond to the bifurcation points for equilateral and isosceles *LRE* for $\nu = 1$. The other point $(\sigma, \sigma_3) = (0.3202\dots\pi, 0.5388\dots\pi)$ is new. The mass ratio at this point is $\nu_0 = 0.6039\dots$. Numerical calculations suggest that this point is the lower bound for ν , where we can find bifurcation to scalene *LRE* from the 0-*LRE* continuation. In other words, the bifurcation of this type occurs for $\nu_0 < \nu < 1$. The reason is the following. At $\nu = 8(36 - \sqrt{3})/333$, the scalene continuation is a loop. This means that two surfaces of $\tilde{\lambda}_{12} = 0$ and $\lambda_{23} = 0$ intersect, and the intersection curve is a loop. Numerical calculation shows that smaller ν makes smaller loop, and at the limit $\nu \rightarrow \nu_0$ the loop becomes just a point $(0.3202\dots\pi, 0.5388\dots\pi)$. Namely, the two surfaces just touch at this point. Thus the lower bound for ν in order to have this kind of bifurcation is $\nu_0 = 0.6039\dots$

5 *LRE* with general masses

In this section, we will tackle the case of general masses. Remember that if the three masses are not equal, by Corollary 1, the shapes for the *LRE* are scalene triangles.

5.1 Continuation from Lagrangian equilateral *RE* on \mathbb{R}^2 to *LRE* on \mathbb{S}^2

Let s_k be the arc length between the masses m_i and m_j , where $(i, j, k) = (1, 2, 3), (2, 3, 1), (3, 1, 2)$. Then $\sigma_k = s_k/R$, where R is the radius of \mathbb{S}^2 . The Euclidean limit where the Lagrange equilateral solution exists is achieved by taking $R \rightarrow \infty$.

Proposition 8. *The Lagrange equilateral solution when R goes to infinity exists, and the continuation to finite R also exists.*

Proof. The limit $R \rightarrow \infty$ of the conditions $\lambda_{12} = \lambda_{23} = 0$ are

$$\frac{(s_1^3 - s_2^3) \sum_k m_k s_k^3}{s_1^3 s_2^3} = \frac{(s_2^3 - s_3^3) \sum_k m_k s_k^3}{s_2^3 s_3^3} = 0. \quad (33)$$

The solution is $s = s_k$, $k = 1, 2, 3$, which corresponds to the equilateral *LRE*.

Then, for $R \rightarrow \infty$,

$$R^{-2} \nabla \lambda_{12} \times \nabla \lambda_{23} \Big|_{\sigma_k = s/R} \rightarrow \frac{9(m_1 + m_2 + m_3)^2}{s^2} (1, 1, 1) \neq 0. \quad (34)$$

By the implicit function theorem, the continuation of equilateral *LRE* to finite R exists. \square

The above result was first proved in [1], by using a different approach.

Proposition 9. *The continuation of equilateral LRE in \mathbb{R}^2 to \mathbb{S}^2 with finite R has $\sigma_i < \sigma_j < \sigma_k$ if $m_i < m_j < m_k$.*

Proof. Let be $\sum_{\ell=1,2,3} \sigma_\ell = \sum_{\ell=1,2,3} s_\ell / R = 3\epsilon \ll 1$. Then the expansion of σ_ℓ to $O(\epsilon^3)$ is

$$\sigma_\ell = \epsilon + \left(\frac{m_\ell}{m_1 + m_2 + m_3} - \frac{1}{3} \right) \frac{\epsilon^3}{3!} + O(\epsilon^5). \quad (35)$$

Therefore, $\sigma_i < \sigma_j < \sigma_k$ if $m_i < m_j < m_k$ for sufficiently small σ . By Proposition 1, the ordering of σ_ℓ cannot be changed in the continuation of the solution. Therefore, the ordering $\sigma_i < \sigma_j < \sigma_k$ is preserved in the continuation to finite size of σ . \square

Remark 4. *For finite R , there are no equilateral solutions if the masses are not equal. Instead, there are almost equilateral solutions if $\sigma_\ell \ll 1$. Similarly, there are three continuations of ERE which are almost similar to the three Euler solutions on the Euclidean plane \mathbb{R}^2 [11]. We call such continuation of the solutions as “0-LRE continuation” and “0-ERE continuations” respectively, because these continuations start from the origin.*

5.2 Continuation of Euler RE on the equator to Lagrange RE

If the masses satisfy the condition (12), then ERE on the equator exists.

Proposition 10. *The continuation of LRE from an ERE on the equator exists.*

Proof. Direct calculation shows that $\lambda_{12} = \lambda_{23} = 0$ are satisfied by σ_k in (13). Besides that, we get

$$\begin{aligned} & m_1^2 m_2^2 m_3^2 (1, 1, 1) \cdot (\nabla \lambda_{12} \times \nabla \lambda_{23}) \\ &= - \left(\sum_k m_k^2 \right) \left(\sum_\ell \mu_\ell \right) (\mu_1 + \mu_2 - \mu_3)(\mu_2 + \mu_3 - \mu_1)(\mu_3 + \mu_1 - \mu_2) \\ &\neq 0 \text{ by the condition (12).} \end{aligned} \quad (36)$$

By the implicit function theorem, we get the result. \square

Proposition 11. *The continuation of LRE from the ERE on the equator has $\sigma_i < \sigma_j < \sigma_k$ if $m_i < m_j < m_k$.*

Proof. Without loss of generality, we can assume that $m_1 < m_2 < m_3$. Since $\mu_k = \sqrt{m_1 m_2 m_3} / \sqrt{m_k}$ for $k = 1, 2, 3$, $\mu_1 > \mu_2 > \mu_3$ is obvious. Then $\cos \sigma_i - \cos \sigma_j = (\mu_i - \mu_j) \left((\mu_i + \mu_j)^2 - \mu_k^2 \right) / (2\mu_1 \mu_2 \mu_3)$ for $(i, j, k) = (1, 2, 3)$, $(2, 3, 1)$, and $(3, 1, 2)$ yields $\cos \sigma_1 > \cos \sigma_2 > \cos \sigma_3$, because any ERE on the equator satisfies $\mu_i + \mu_j > \mu_k$. Since $\cos \sigma$ is a decreasing function in $0 < \sigma < \pi$, the proposition is proved. \square

5.3 Mass ratio for a given shape

To go further into the consideration of the bifurcation of LRE and ERE for general masses, we treat the conditions for LRE, $\lambda_{12} = \lambda_{23} = 0$, as the equations for the mass ratios $\nu_1 = m_1/m_3$ and $\nu_2 = m_2/m_3$. This subsection is an extension of the section 4.1.1 for partial equal masses case to the general masses case.

The conditions $\lambda_{12} = \lambda_{23} = 0$ take the form

$$S \begin{pmatrix} \nu_1 \\ \nu_2 \\ 1 \end{pmatrix} = 0, \quad (37)$$

where S is a two by three matrix in function of σ_k . The rank of S is at most two.

If $\text{rank } S = 2$, (ν_1, ν_2) is determined uniquely. Let be

$$\tilde{S} = \begin{pmatrix} S_{11} & S_{12} \\ S_{21} & S_{22} \end{pmatrix}, \quad s = \begin{pmatrix} S_{13} \\ S_{23} \end{pmatrix} \quad (38)$$

Then

$${}^t(\nu_1, \nu_2) = -\tilde{S}^{-1}s. \quad (39)$$

The following lemmas are obvious.

Lemma 1. *For a given shape σ_k , if $\text{rank } S = 2$ and if the equation ${}^t(\nu_1, \nu_2) = -\tilde{S}^{-1}s$ gives $\nu_1 > 0$ and $\nu_2 > 0$, then this shape form a LRE with this mass ratio.*

Remark 5. *We have checked the shapes in U_{phys} with $\sigma_k \in \{\ell\pi/12, 1 \leq \ell < 12\}$ and $\sigma_1 \leq \sigma_2 \leq \sigma_3$. There are 73 LRE among the total of 133 such grid points. All of them have $\det \tilde{S} > 0$. There are 25 scalene LRE. For example $(\sigma_1, \sigma_2, \sigma_3) = (\pi/4, 3\pi/4, 5\pi/6)$ has $\det \tilde{S} = 1/4$, $(\nu_1, \nu_2) = ((2 + 3\sqrt{3})/2, (-2 + 5\sqrt{3})/2)$, and $\lambda = 2(2 + \sqrt{3})$.*

Lemma 2. For a given shape σ_k , if $\text{rank } S = \text{rank } \tilde{S} = 1$ and there are solutions $\nu_k > 0$ that satisfy $S_{11}\nu_1 + S_{12}\nu_2 + S_{13} = 0$, then this shape form a RE with these mass ratios.

5.4 Bifurcations between ERE on a rotating meridian and LRE

If there is a bifurcation point between an ERE on a rotating meridian and a LRE, it must be on the plane $\sigma_k = \sigma_i + \sigma_j$. Without loss of generality, we can take the plane $\sigma_3 = \sigma_1 + \sigma_2$.

5.4.1 Bifurcation points on the plane $\sigma_3 = \sigma_1 + \sigma_2$

The aim of this subsection is to prove the following result.

Theorem 2. Any point on the curve

$$h = \cos(3\sigma_3) - 3\cos(\sigma_3) + 2\cos(2\sigma_3)\cos(\sigma_1 - \sigma_2) = 0 \quad (40)$$

which belongs to the plane $\sigma_3 = \sigma_1 + \sigma_2$ is a bifurcation point of ERE on a rotating meridian and a LRE for continuously many (ν_1, ν_2) . Inversely, if a continuation of LRE (for given $\nu_1, \nu_2 > 0$) reaches the $\sigma_3 = \sigma_1 + \sigma_2$ plane, the point is on the curve $h = 0$. Therefore, this is a bifurcation point between LRE and ERE.

The proof of this Theorem is given in a sequence of lemmas.

Lemma 3. On the plane $\sigma_3 = \sigma_1 + \sigma_2$, $\text{rank } S = \text{rank } \tilde{S} = 1$ on the curve $h = 0$, otherwise $\text{rank } S = \text{rank } \tilde{S} = 2$.

Proof. A direct calculation shows that

$$(S_{11}, S_{12}, S_{13}) \times (S_{21}, S_{22}, S_{23}) = \left(\frac{\sin \sigma_2}{\sin \sigma_1}, \frac{\sin \sigma_1}{\sin \sigma_2}, -\frac{\sin \sigma_1 \sin \sigma_2}{\sin \sigma_3} \right) \frac{h}{2}. \quad (41)$$

Since $0 < \sigma_1, \sigma_2, \sigma_3 < \pi$, this vector is null if and only if $h = 0$. \square

Lemma 4. The curve $h = 0$, for $0 < \sigma_1 + \sigma_2 = \sigma_3 < \pi$, is a continuous curve that connects $(\sigma_1, \sigma_2) = (0, \pi/2)$ and $(\pi/2, 0)$. The range of σ_3 is $\pi/2 < \sigma_3 \leq 2\sigma_E = \arccos(-1 + 1/\sqrt{2}) < 3\pi/4$.

Proof. Since $0 < 2\sigma_3 < 2\pi$, the solutions of $\cos(2\sigma_3) = 0$ are $2\sigma_3 = \pi/2, 3\pi/2$. But $3\cos(\sigma_3) - \cos(3\sigma_3) = \pm 2\sqrt{2} \neq 0$ on these points. Therefore $\cos(2\sigma_3) \neq 0$ on $h = 0$. Then

$$\cos(\sigma_1 - \sigma_2) = \frac{3\cos(\sigma_3) - \cos(3\sigma_3)}{2\cos(2\sigma_3)}. \quad (42)$$

Since

$$\frac{d}{d\sigma_3} \left(\frac{3\cos(\sigma_3) - \cos(3\sigma_3)}{2\cos(2\sigma_3)} \right) = \frac{(9 + 4\cos(2\sigma_3) + \cos(4\sigma_3))\sin(\sigma_3)}{2\cos^2(2\sigma_3)} > 0, \quad (43)$$

$\cos(\sigma_1 - \sigma_2)$ is a strictly increasing function of σ_3 . Therefore, the upper limit of σ_3 is given by $3\cos(\sigma_3) - \cos(3\sigma_3) = 2\cos(2\sigma_3)$. The solution is $\sigma_3 = 2\sigma_E$ and $\sigma_1 = \sigma_2 = \sigma_E$. Decreasing σ_3 , there are two solutions of (σ_1, σ_2) . At $\sigma_3 = \pi/2$, $\cos(\sigma_1 - \sigma_2) = 0$, and $(\sigma_1, \sigma_2) = (0, \pi/2)$ and $(\pi/2, 0)$. For $\sigma_3 < \pi/2$ the solution (σ_1, σ_2) are out of $0 < \sigma_1, \sigma_2$. Therefore, the range of σ_3 is $\pi/2 < \sigma_3 \leq 2\sigma_E$. \square

Lemma 5. *On the plane $\sigma_3 = \sigma_1 + \sigma_2$, we can find positive mass ratios that satisfy the conditions $\lambda_{12} = \lambda_{23} = 0$ only on the curve $h = 0$. Outside of this curve, the conditions demand $\nu_1, \nu_2 < 0$.*

Proof. On the curve $h = 0$, $\text{rank } S = \text{rank } \tilde{S} = 1$, the solutions are given by,

$$\begin{aligned} \nu_2 = \nu_1 & \frac{1 - \cos(\sigma_3)\sin^3(\sigma_1)/\sin^3(\sigma_2)}{1 - \cos(\sigma_3)\sin^3(\sigma_2)/\sin^3(\sigma_1)} \\ & + \frac{\left(\cos(\sigma_2)/\sin^3(\sigma_1) - \cos(\sigma_1)/\sin^3(\sigma_2)\right)\sin^3(\sigma_3)}{1 - \cos(\sigma_3)\sin^3(\sigma_2)/\sin^3(\sigma_1)}. \end{aligned} \quad (44)$$

As shown above $\cos(\sigma_3) < 0$ on $h = 0$, therefore the coefficient of ν_1 in equation (44) is always positive; whereas the constant term could be positive, zero or negative. Therefore, for any point on $h = 0$, we can always take positive ν_1 and ν_2 .

On the other hand, at (σ_1, σ_2) where $h \neq 0$, $\text{rank } S = 2$. Therefore, ν_1, ν_2 are determined uniquely. A direct calculation shows that both are negative,

$$\nu_1 = -\sin^2(\sigma_3)/\sin^2(\sigma_1), \quad \nu_2 = -\sin^2(\sigma_3)/\sin^2(\sigma_2). \quad (45)$$

\square

Remark 6. *As shown in (44), continuously many (ν_1, ν_2) share the same (σ_1, σ_2) on $h = 0$.*

Lemma 6. *The shape $\sigma_3 = \sigma_1 + \sigma_2$ on $h = 0$ with the mass ratios given by equation (44) satisfies the condition for ERE.*

Proof. The condition for ERE with $\sigma_3 = \sigma_1 + \sigma_2$ is given by equation (11). Substitution of the relation (44) into (11) yields

$$d = \sin(\sigma_1 - \sigma_2) h r = 0 \quad \text{on} \quad h = 0. \quad (46)$$

Where

$$r = \frac{\cos(\sigma_3)(1 - \cos(2\sigma_3) + \nu_1(1 - \cos(2\sigma_1))(\cos(\sigma_3) - \cos(2\sigma_3)\cos(\sigma_1 - \sigma_2))}{4(1 - \cos(\sigma_3)\sin^3(\sigma_2)/\sin^3(\sigma_1))\sin^4(\sigma_1)\sin^2(\sigma_2)\sin^2(\sigma_3)} \quad (47)$$

is finite on $h = 0$ because $\cos(\sigma_3) < 0$. \square

Lemma 7. *For a given point (σ_1, σ_2) on $h = 0$ and $\nu_1, \nu_2 > 0$ which are related by equation (44), the continuation of ERE from this point exists.*

Proof. The substitution of ν_2 given by equation (44) into $\nabla d = (\partial_{\sigma_1}, \partial_{\sigma_2})d$ gives

$${}^t(\nabla d) = M \begin{pmatrix} \nu_1 \\ 1 \end{pmatrix}, \quad (48)$$

where M is a two by two matrix of functions of (σ_1, σ_2) . Now, a direct calculation using $h = 0$ yields

$$\det M = \frac{8 \sin(\sigma_1 - \sigma_2) \sin^5(\sigma_3)(3 + 3 \cos(2\sigma_3) + \cos(4\sigma_3))}{\cos^2(2\sigma_3) \sin^4(\sigma_1) \sin^4(\sigma_2)(1 - \cos(\sigma_3) \sin^3(\sigma_2)/\sin^3(\sigma_1))} \quad (49)$$

$\neq 0$ on $h = 0$ and $\sigma_1 \neq \sigma_2$.

Therefore, if $\sigma_1 \neq \sigma_2$, $\nabla d \neq 0$. By the implicit function theorem, there is a continuation of ERE from this point.

For the case $\sigma_1 = \sigma_2$, we know from by Proposition 1 that $m_1 = m_2$. The existence of the continuation of ERE with $\sigma_1 = \sigma_2$ is obvious. \square

Lemma 8. *For a given point (σ_1, σ_2) on $h = 0$ and $\nu_1, \nu_2 > 0$ that are related by equation (44), the continuation of LRE from this point exists.*

Proof. Consider $c = \nabla \lambda_{12} \times \nabla \lambda_{23}$ at the point (σ_1, σ_2) , where $\nabla = (\partial_{\sigma_1}, \partial_{\sigma_2}, \partial_{\sigma_3})$. Substituting ν_2 given by equation (44), we obtain that each component of c

has the form $c_i = a_{i1}\nu_1^2 + a_{i2}\nu_1 + a_{i3}$, where the a_{ij} are functions of (σ_1, σ_3) . Namely,

$$A \begin{pmatrix} \nu_1^2 \\ \nu_1 \\ 1 \end{pmatrix} = c. \quad (50)$$

Substituting $\sigma_3 = \sigma_1 + \sigma_2$ and using $\cos(\sigma_1 - \sigma_2)$ in (42), we get

$$\det A = \frac{\sin^{10}(\sigma_3)}{4 \sin^7(\sigma_1) \sin^7(\sigma_2) \cos^2(2\sigma_3)} \frac{\sin(\sigma_1 - \sigma_2) n}{(1 - \cos(\sigma_3) \sin^3(\sigma_2) / \sin^3(\sigma_1))^3}, \quad (51)$$

where

$$n = -710 - 1108 \cos(2\sigma_3) - 449 \cos(4\sigma_3) - 100 \cos(6\sigma_3) + 6 \cos(8\sigma_3) + 8 \cos(10\sigma_3) + \cos(12\sigma_3). \quad (52)$$

We can show that $n \neq 0$ on $h = 0$ by a simple calculation.

Therefore, $c \neq 0$ if $\sigma_1 \neq \sigma_2$. By the implicit function theorem, there is a continuation of *LRE* from this point.

For the case $\sigma_1 = \sigma_2$, we obtain $m_1 = m_2$ by Proposition 1. For this case, $\sigma_1 = \sigma_2 = \sigma_E$. The existence of the continuation of *LRE* from this point is shown in Proposition 7. \square

The lemmas 3 to 8 prove Theorem 2.

5.4.2 Number of bifurcation points on $\sigma_3 = \sigma_1 + \sigma_2$ for given mass ratio

In the previous Theorem we showed that any point on the curve $h = 0$ located on the plane $\sigma_3 = \sigma_1 + \sigma_2$ is a bifurcation point between *ERE* and *LRE* for continuously many (ν_1, ν_2) .

Then for given (ν_1, ν_2) , how many bifurcation points exist on the plane, and what (σ_1, σ_2) if exist? In this subsection, we will give an equation to count the number, and to find the position.

Substituting (42) into (44), we get

$$\sin \Delta = \frac{-\delta\nu \left(16 + 11 \cos(2\sigma_3) + \cos(6\sigma_3) \right) \sin(\sigma_3)}{2 \cos(2\sigma_3) \left((1 + \cos(4\sigma_3)) - \nu(5 + 4 \cos(2\sigma_3) + \cos(4\sigma_3)) \right)}, \quad (53)$$

where $\Delta = \sigma_2 - \sigma_1$, $\nu = (\nu_1 + \nu_2)/2$ and $\delta\nu = (\nu_2 - \nu_1)/2$. Then, $1 - \cos^2(\Delta) = \sin^2(\Delta)$ with (42) for $\cos \Delta$ will determine σ_3 . Then $\sin \Delta$ and $\cos \Delta$ will determine σ_1 and σ_2 .

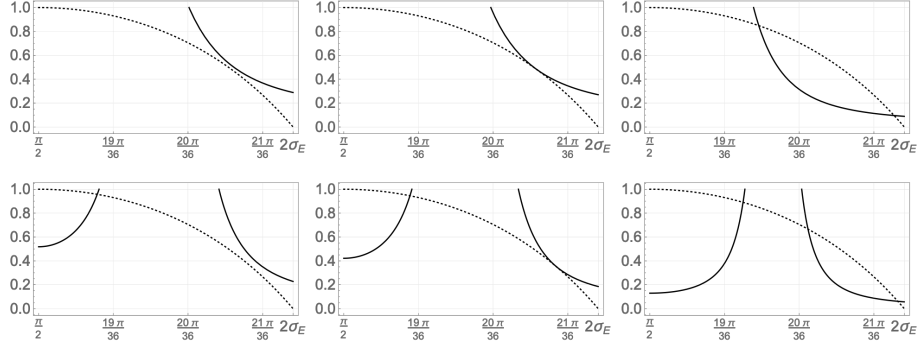


Figure 6: The dashed curve and solid curve represents $1 - \cos^2(\Delta)$ and $\sin^2(\Delta)$ respectively, the horizontal axis is σ_3 . Upper row from left to right: $(\nu, \delta\nu)$ are $(1, 0.09)$, $(1, 0.0870\dots)$, $(1, 0.05)$. The number of bifurcation points (intersections) are 0, 1, 2. Lower row from left to right: $(\nu, \delta\nu) = (11/12, 0.06)$, $(11/12, 0.0541\dots)$, $(11/12, 0.03)$. The number of bifurcation points are 1, 2, 3.

Note that $1 - \cos^2(\Delta)$ with (42) is a decreasing function of σ_3 , which takes the value 1 for $\sigma_3 = \pi/2$ and 0 for $\sigma_3 = 2\sigma_E$. On the other hand, $\sin^2(\Delta) = (\delta\nu)^2/(1 - \nu)^2$ for $\sigma_3 = \pi/2$ and $(13 + 16\sqrt{2})\delta\nu^2/(2 - 3\nu)^2$ for $\sigma_3 = 2\sigma_E$. Therefore, it may have 0, 1, 2 or 3 solutions of σ_3 .

Then, we get the following lemma.

Lemma 9. *For the case $|\delta\nu| < |1 - \nu|$, there is at least one bifurcation point between LRE and ERE on the plane $\sigma_3 = \sigma_1 + \sigma_2$, $\pi/2 < \sigma_3 \leq 2\sigma_E$.*

Proof. The denominator of $\sin \Delta$ has zero if $2/3 \leq \nu \leq 1$. If ν is outside of this range, the result is obvious because $\sin \Delta$ is a continuous function. If ν is in this range, the function $\sin^2(\Delta)$ is not continuous but goes to plus infinity at the point. Therefore, the equation $1 - \cos^2(\Delta) = \sin^2(\Delta)$ has at least one solution. \square

Then, the following result is obvious.

Proposition 12. *For $m_i < m_j < m_k$, there is at least one bifurcation point of LRE and ERE on the plane $\sigma_k = \sigma_i + \sigma_j$, $\pi/2 < \sigma_k \leq 2\sigma_E$.*

Proof. Without loss of generality, we can assume $m_1 < m_2 < m_3$. Then $m_2 - m_1 < 2m_3 - (m_1 + m_2)$, namely $|\delta\nu| < |1 - \nu|$ is satisfied. \square

5.5 Numerical Results

Figure 6 shows examples of $(\nu, \delta\nu)$ that give 0, 1, 2, 3 bifurcation points. Although the case $(\nu, \delta\nu) = (1, 0.09)$ has no bifurcation point on the plane $\sigma_3 = \sigma_1 + \sigma_2$, it has the bifurcation point on the plane $\sigma_2 = \sigma_3 + \sigma_1$ by Proposition 12 because m_2 is the heaviest for this case.

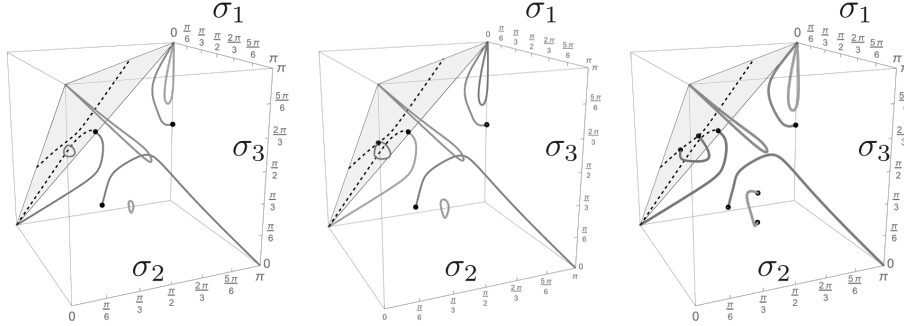


Figure 7: Continuations of LRE on \mathbb{S}^2 for $(\nu, \delta\nu) = (11/12, 0.06)$ (left), $(11/12, 0.0541\dots)$ (middle) and for $(11/12, 0.03)$ (right). They correspond to the lower diagrams in Figure 6. Solid curves represents the continuations of LRE . There are seven continuations of LRE . The black balls represent bifurcation points between LRE and ERE . The grey plane corresponds to $\sigma_3 = \sigma_1 + \sigma_2$ and the dashed curves on this plane are ERE . We observe one bifurcation point between LRE and ERE on this plane (subfigure in the left side), two (subfigure in the middle), and three (subfigure in the right side).

The corresponding continuations of LRE for $(\nu, \delta\nu) = (11/12, 0.06)$, $(11/12, 0.0541\dots)$, and $(11/12, 0.03)$ are shown in Figure 7. The grey plane corresponds to $\sigma_3 = \sigma_1 + \sigma_2$. Left: At $(\nu, \delta\nu) = (11/12, 0.06)$, there is only one bifurcation point between 0- LRE and 0- ERE . As you can see in Fig. 7, there is a small loop near the plane, which does not reach the plane. Therefore, the loop doesn't yields a bifurcation point. As $\delta\nu$ is smaller, the loop is larger. Middle: When $\delta\nu = 0.0541\dots$, the loop touches the plane at one point, which is a new bifurcation point. Thus, there are two bifurcation points for $(11/12, 0.0541\dots)$ as shown in Figure 6. The bifurcated ERE is different from the 0- ERE . Decreasing $\delta\nu$ the loop gets bigger and then intersects the plane. Right: Thus, we have three bifurcation points at $(11/12, 0.03)$.

In Figure 7, another similar small loop (left) and open arc (right) which bifurcate to ERE on the plane $\sigma_2 = \sigma_3 + \sigma_1$ is shown.

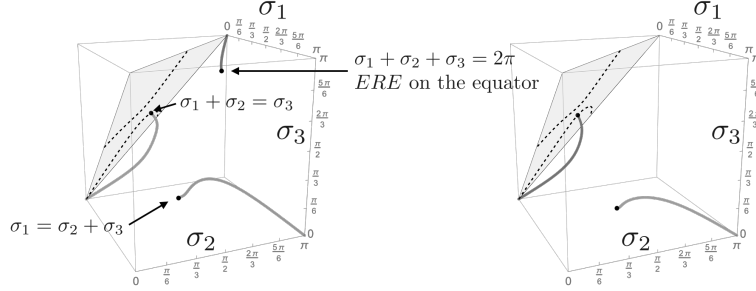


Figure 8: Continuations of *LRE* and continuations of *ERE* on $\sigma_3 = \sigma_1 + \sigma_2$ plane. Left: For $m_1 : m_2 : m_3 = 1 : 2 : 4$, namely $(\nu, \delta\nu) = (3/8, 1/8)$. The continuation from $(0, \pi, \pi) \in U$ ends at the *ERE* on the equator. Right: For $m_1 : m_2 : m_3 = 1 : 2 : 12$, $(\nu, \delta\nu) = (1/8, 1/24)$. At this mass ratio there is no *ERE* on the equator. So there is no continuation from it.

The continuation which starts at $(\pi, \pi, 0) \in U$ bifurcates to *ERE* on $\sigma_1 = \sigma_2 + \sigma_3$. The end point of the continuation that starts at $(0, \pi, \pi) \in U$ is *ERE* on the equator.

We see other two loops that start and end at $(0, \pi, \pi)$ or $(\pi, 0, \pi)$. They are elements of the seven continuations in Figure 7, where the mass ratios $m_1 : m_2 : m_3$ are not so far from $1 : 1 : 1$.

Figure 8 shows the continuations for $m_1 : m_2 : m_3 = 1 : 2 : 4$ and $1 : 2 : 12$. No loop continuations are seen. Three continuations exist for $m_1 : m_2 : m_3 = 1 : 2 : 4$. On the other hand, since the mass ratio $1 : 2 : 12$ does not satisfy the condition for *ERE* on the equator (12), the *ERE* and the continuation of *LRE* from this point does not exist. Thus, there are only two continuations of *LRE*.

The numerical experiments show a couple of interesting properties of the continuation of *LRE*, *ERE*, and the bifurcation between them.

(1) The 0-*LRE* continuation and one of the 0-*LRE* continuations are directly connected by the bifurcation point. The 0-*LRE* continuation reaches the plane $\sigma_3 = \sigma_1 + \sigma_2$, then bifurcates to *ERE*, where m_3 (the heaviest mass) is placed in the middle, Then it continues back to the 0-*ERE* continuation keeping m_3 (the heaviest mass) in the middle. See Figures 7 and 8. Note that Proposition 12 ensures the existence of such bifurcation point between a *LRE* and an *ERE* continuations, but not ensures that the continuations are 0-*LRE* and 0-*ERE*.

(2) There are at most 7 continuations of *LRE*. Among them, the 0-*LRE* continuation and the continuation of *LRE* from *ERE* on the equator

sharing the same ordering of σ_ℓ , namely $\sigma_1 < \sigma_2 < \sigma_3$ if $m_1 < m_2 < m_3$ by Propositions 9 and 11. The other 5 continuations have mutually different ordering. Therefore, all possible 6 orderings of σ 's are realised by the 7 continuations.

6 Conclusions and final comments

The variables $(\sigma_1, \sigma_2, \sigma_3) \in U_{\text{phys}}$ for having *LRE* on \mathbb{S}^2 is determined by the two conditions $\lambda_{12} = \lambda_{23} = 0$. Therefore, *LRE* have one-dimensional intersection curve, namely one-dimensional continuation, in general. Similarly, *ERE* on \mathbb{S}^2 have one-dimensional continuation.

We have proved the local existence of the continuations. The proof for the global existence of such continuation still need a better understanding of the surfaces defined by $\lambda_{ij} = 0$.

Special attention was paid to the 0-*LRE* continuation. On the Euclidean plane \mathbb{R}^2 , there are two isolated Lagrangian equilateral configurations that have opposite orientation, and three isolated Euler configurations. We have shown that on \mathbb{S}^2 , with almost all mass ratios, the 0-*LRE* continuation (two almost equilateral configurations with opposite orientations) and one 0-*ERE* continuation, where the heaviest mass is placed between the other two masses, are connected by the continuations via bifurcation(s). See Figure 9. This is true for the mass ratios $m_i \leq m_j < m_k$ and $m_i = m_j = m_k$, but not true for $m_i < m_j = m_k$. See the $\nu > 1$ continuation in Figure 3.

When we say that there are two Lagrange equilateral solutions in the planar three-body problem, we count the similarity class of the shapes under rotations and homotheties. Since we don't have these similarity classes on \mathbb{S}^2 , we have continuously many *LRE* as shown in Figure 9. However, the counting based on similarity has not much meaning to compare the number of solutions on \mathbb{S}^2 and Euclidean \mathbb{R}^2 .

It is better to count the number of *RE* on the basis of continuity instead of similarity. Because the similar shape $r_{ij} = \lambda a_{ij}$ with fixed a_{ij} and scaling factor λ is an one dimensional continuation, the continuation is a natural extension of similarity. For the continuation, we have one *LRE* in the space r_{ij} , and two in the configuration space counting two orientations. By the same counting, we have at most seven continuations in U_{phys} , and $2 \times 2 \times 7 = 28$ continuations for configurations. Where, the first factor 2 counts the orientations, and the second 2 counts whether the placement is in the northern or southern hemisphere ($s = \pm 1$ in equation (9)).

In this article we have considered only positive masses. Some authors

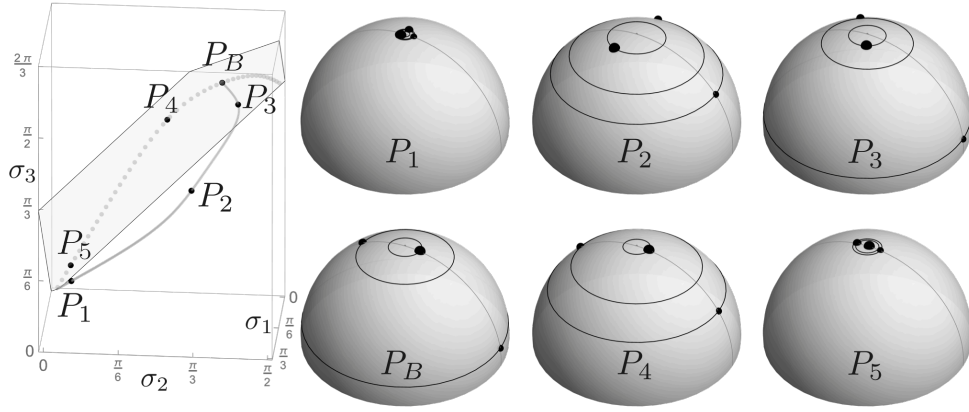


Figure 9: Two continuations from the neighbour of the origin in U_{phys} (left), i.e. the 0-*LRE* continuation and 0-*ERE* continuation, and the corresponding configurations (right), for the mass ratios $m_1 : m_2 : m_3 = 1 : 2 : 4$. The points P_1, P_2, P_3 and P_B, P_4, P_5 represents *LRE* and *ERE* respectively. The point P_B is the bifurcation point between *LRE* and *ERE*. Left: The solid and dotted curve represents the 0-*LRE* continuation and 0-*ERE* continuation respectively. The grey plane is $\sigma_3 = \sigma_1 + \sigma_2$ plane. Right: The configurations on the northern hemisphere. The meridian of $\phi = 0$ and π are shown. The smallest and the biggest black points represents m_1 and m_3 . The mass m_1 is placed on $\phi = 0$. The circles are the orbits of the three bodies.

have studied the case for two positive masses and a third massless particle, called the restricted three body problem on \mathbb{S}^2 , see for instance [12, 15]. An interesting question is try to extend our results to the restricted problem. In this paper we have analyzed just the restricted isosceles *LRE* on the sphere, that is, we consider $m_1 = m_2 > 0$ and $m_3 = 0$ (see subsection 4.1.3). We showed that our results cover this particular case. We pointing out that in this case, there are values of σ_3 not allowed for having *LRE*, size shape dependence is interesting. However we are far to have a complete analysis of the general restricted three body problem on the sphere. It will be part of another paper.

Another important question is about the stability of the relative equilibria that we found in this work. To tackle this problem we need to use geometric mechanics techniques as for instance in [2], we will do this in a future work. Last but not least, we point out that by using our techniques, we can also study the relative equilibria for the vortex problem on the sphere as in [3].

Acknowledgements

The authors of this paper thank to the anonymous reviewer for his/her comments and suggestions, which help us to improve the manuscript. The second author (EPC) has been partially supported by Asociación Mexicana de Cultura A.C. and Conacyt-México Project A1S10112.

References

- [1] Bengochea A., García-Azpeitia C., Pérez-Chavela E., Roldan P. *Continuation of relative equilibria in the n-body problem to spaces of constant curvature* Journal of Differential Equations, **307**, (2022), 137–159.
- [2] Bolsinov A.V., Borisov A. V., Mamaev I. S., *The bifurcation analysis and the Conley Index in Mechanics*, Regular and Chaotic Dynamics **17-5**, (2012), 457–478.
- [3] Bolsinov A.V., Borisov A. V., Mamaev I. S., *Lie algebras in vortex dynamics and celestial mechanics*, Regular and Chaotic Dynamics **4-1**, (1999), 23–50.
- [4] Borisov A.V., Mamaev I.S., Bizyaev I.A. *The Spatial Problem of 2 Bodies on a Sphere, Reduction and Stochasticity* , Regular and Chaotic Dynamics **216-5**, (2016), 556–580.

- [5] Borisov A. V., Mamaev I. S., Kilin A. A., *Two-body problem on a sphere: reduction, stochasticity, periodic orbits*; Institute of Computer Science, Udmurt State University, (2005).
- [6] Diacu F., Pérez-Chavela E., Santoprete M., *The n-body problem in spaces of constant curvature. Part I: Relative equilibria*. J. Nonlinear Sci. **22** (2012), no. 2, 247–266.
- [7] Diacu F., *Relative equilibria of the curved N-body problem*. Atlantis Studies in Dynamical Systems, Atlantis Press, Amsterdam, Paris, Beijing **1**, 2012.
- [8] Diacu F. and Pérez-Chavela E., *Homographic solutions of the curved 3-body problem*, Journal of Differential Equations **250**, (2011), 340–366.
- [9] Diacu F., Zhu S., *Almost all 3-body relative equilibria on S^2 and \mathbb{H}^2 are inclined*. Discrete and Continuous Dynamical Systems, Series S **13-4** (2020), 1131–1143.
- [10] Euler L. *De mutuo rectilineo trium corporum se mutuo attrahentium*, Novi Comm. Acad. Sci. Imp. Petrop. 11 (1767) 144–151.
- [11] Fujiwara T. and Pérez-Chavela E. *Three-Body Relative Equilibria on S^2* , Regular and Chaotic Dynamics **28**, Nos. 4–5, (2023), 686–702.
- [12] Kilin A. A. *Libration points in spaces S^2 and L^2* , Regular and Chaotic Dynamics **4-1**, (1999), 91–103.
- [13] Koslov, V.V. *Dynamics in spaces of constant curvature*, Moscow Univ. Math: Bull. **49-2**, (1994), 21–28.
- [14] Marsden J., Weinstein A. *Reduction of symplectic manifolds with symmetry*, Reports on mathematical physics **5-1**, (1974), 121-130.
- [15] Martínez R., Simó C. *Relative equilibria of the restricted three-body problem in curved spaces*, Celestial Mechanics and Dynamical Astronomy **128**, (2017), 221–259.
- [16] Lagrange J.L., *Essais sur the probleme des trois corps*. Paris, France (1772).
- [17] Moeckel R., Notes on Celestial Mechanics (especially central configurations). <http://www.math.umn.edu/~moeckel/notes/Notes.html>

- [18] Pérez-Chavela E. and Reyes-Victoria J.G., *An intrinsic approach in the curved n -body problem. The positive curvature case*, Trans. Amer. Math. Soc. **364**-7, (2012), 3805–3827.
- [19] Pérez-Chavela E. and Sánchez-Cerritos J.M. *Euler-type relative equilibria in spaces of constant curvature and their stability*, Canad. J. Math. **70**-2, (2018), 426–450.
- [20] Shchepetilov A.V., *Nonintegrability of the two-body problem in constant curvature spaces*. J. Phys. A **39** (2006), no. 20, 5787–5806.
- [21] Tibboel P., *Polygonal homographic orbits in spaces of constant curvature*. Proc. Amer. Math. Soc. **141** (2013), 1465–1471
- [22] Wintner A., *The Analytical Foundations Celestial of Mechanics*, Princeton University Press, Princeton, New York, (1941).
- [23] Zhu S., *Eulerian relative equilibria of the curved 3-body problem*. Proc. Amer. Math. Soc. **142** (2014), 2837–2848.